

# A computerized tomography based deep learning diagnostic method of maxillary sinus fungal balls

L. Peng<sup>1</sup>, Q. Wu<sup>2</sup>, R. Shi<sup>2</sup>, H. Kong<sup>3</sup>, W. Li<sup>4</sup>, W. Duan<sup>1</sup>, L. Zhu<sup>1\*</sup>

<sup>1</sup>Department of Otolaryngology, Shanghai University of Medicine & Health Sciences Affiliated Zhoupu Hospital, Shanghai 201318, China

<sup>2</sup>Department of Otolaryngology Head and Neck Surgery, Shanghai 9th People's Hospital/Shanghai Ninth People's Hospital, School of medicine, Shanghai Jiao Tong University, Shanghai 200011, China

<sup>3</sup>Inspection Technology Laboratory, Intelligent Manufacturing Research Center of Midea Group, Shanghai 201702, China

<sup>4</sup>Department of Radiology, Shanghai University of Medicine & Health Sciences Affiliated Zhoupu Hospital, Shanghai 201318, China

## ► Original article

## ABSTRACT

### \*Corresponding author:

Lixin Zhu,

E-mail: zhulx2008@163.com

Received: September 2023

Final revised: October 2023

Accepted: October 2023

Int. J. Radiat. Res., January 2024;  
22(1): 9-15

DOI: 10.52547/ijrr.21.1.2

**Keywords:** Maxillary sinus, fungal ball, computed tomography, deep learning, convolutional neural network.

**Background:** Traditional diagnostic methods are limited in accuracy when detecting maxillary sinus fungal balls, leading to a higher risk of misdiagnosis or missed diagnosis. This study focuses on a deep learning-based algorithm for assisting in the localization and diagnosis of maxillary sinus fungal balls, addressing the limitations of conventional diagnostic procedures. **Materials and Methods:** Axial CT imaging data of maxillary sinus were collected from 107 patients, including 47 cases of maxillary sinus fungal balls, 30 cases of other maxillary sinus lesions and 30 cases of healthy maxillary sinus, based on which, a dataset was constructed and a two-stage assisted diagnosis algorithm consisting of a classification and detection model was established. In the first stage, slices containing maxillary sinus were classified and selected. In the second stage, the selected slices were detected to diagnose and localize the fungal ball lesions in the maxillary sinus. **Results:** The accuracy of the classification model was 92.71%, the mAP and AP50 of the detection model were 0.73 and 0.76, respectively, and the accuracy of the algorithm for the diagnosis of maxillary sinus fungal balls was 84.4%. **Conclusion:** It is feasible to develop a two-stage auxiliary diagnosis method for maxillary sinus fungal ball based on deep learning.

## INTRODUCTION

The incidence of Fungal Rhino-sinusitis (FRS) has been increasing year by year in recent years<sup>(1)</sup>. FRS is a kind of fungal infectious disease of nasal cavity and paranasal sinuses, in which fungus ball is the most common subtype. In clinical practice, fungal balls are most commonly found in the maxillary sinus<sup>(2)</sup>, which is known as maxillary sinus fungal balls. Maxillary Sinus Fungal Balls (MSFBs) are specific infections, and their clinical manifestations are similar to non-specific infections in the maxillary sinus. Non-specific infection of maxillary sinus can be treated conservatively, while fungal ball of maxillary sinus needs surgery, and conservative treatment is usually ineffective. Therefore, early, rapid and accurate diagnosis of fungal ball in maxillary sinus is of great significance for choosing the best treatment scheme and evaluating the prognosis<sup>(3)</sup>.

Currently, Computed Tomography (CT) is the preferred method for preoperative diagnosis of nasosinusitis. However, CT images of some fungal balls in maxillary sinus lack obvious features such as focus, uneven density and calcified focus, and are easily misdiagnosed as non-specific infection of

maxillary sinus and cancer of maxillary sinus<sup>(4,5)</sup>. In addition, manual reading of CT images for diagnosis is often difficult to ensure the accuracy of diagnosis due to differences in doctors' diagnosis and treatment levels<sup>(6)</sup>. At the same time, the low efficiency of manual film reading also increases the burden of patients.

Artificial Intelligence (AI), on the other hand, is increasingly gaining traction in medical image analysis. Image analysis methods based on Deep Learning and Convolutional neural networks (CNN), such as classification<sup>(7,8)</sup>, target detection<sup>(9-11)</sup> and semantic segmentation<sup>(12)</sup>, have been widely explored in various fields of medicine<sup>(13-15)</sup>. This method has a higher accuracy compared to traditional approaches and holds potential applicability in early tumor detection, enhancing diagnostic precision. Kim *et al.*<sup>(16)</sup> used deep learning to establish a diagnostic model for Fahrenheit X-ray images of patients with maxillary sinusitis; Murata *et al.*<sup>(17)</sup> collected panoramic X-rays of healthy subjects and patients with maxillary sinusitis to train the deep learning model. The diagnostic effect of the model was comparable to that of radiologists and significantly better than that of stomatology residents

( $P < 0.01$ ). In the study of fungal ball of maxillary sinus, Xu *et al.* (18) proposed a method of maxillary sinus segmentation, which firstly classified whether the slice contained maxillary sinus, and then segmented maxillary sinus with improved V-Net. Kim *et al.* (19) collected 512 coronal CT images and developed an intelligent classification algorithm for diseases such as fungal balls in the maxillary sinus using ResNet18 based 3D convolutional neural networks. Key slices were screened using 2D CNN and classified by 3D CNN.

However, modeling based on 3D CNN requires a large sample size and high GPU performance requirements, which make the development of algorithm models based on 3D CNN more difficult, and the deployment of models is much limited. Based on 2D CNN and a small amount of maxillary sinus fungal sphere CT image data, this paper constructed 2D maxillary sinus section classification and maxillary sinus fungal sphere detection data set, trained the corresponding classification and detection model, and established a two-stage auxiliary diagnosis method for maxillary sinus fungal sphere. By harnessing the power of computed tomography scans and cutting-edge deep learning technology, we presented an innovative approach to assist in locating and diagnosing maxillary sinus fungal balls. This not only enhances existing diagnostic methods, improving detection accuracy, but also opens up new possibilities for precise diagnosis of maxillary sinus diseases.

## MATERIALS AND METHODS

### Data collection and processing

#### Source of data

This study was approved by the Ethics Committee of Zhoupu Hospital, Pudong New Area, Shanghai. (Approval number: 2022-C-136-E01, review date: 2022-08-11). In this study, CT image data of partial patients who were admitted to AH Otolaryngology Department from January 2018 to October 2021 and BH Otolaryngology Head and Neck Surgery Department from April 2016 to September 2021 were collected, and the case information was desensitized as the basic data of this study.

#### CT scanning method

In this study, axial CT plain scan images with a slice thickness of 1mm were used. The data were collected with the following CT devices: Siemens SOMATOM Definition Flash CT (Germany), Philips Brilliance CT 64 and Brilliance iCT 256 (Holland), GE Revolution CT 256 and Discovery CT 750 HD (America).

The CT images in this study were observed at a window position of 50HU and a window width of 230HU.

### Inclusion and exclusion criteria

**Inclusion criteria of positive group:** All patients underwent CT examination before operation, and histopathology after operation confirmed that the fungus ball involved unilateral or bilateral maxillary sinus. The histopathological sections were treated by paraffin embedding method and HE staining method, and then histological observation was made under microscope.

**Inclusion criteria of negative control group:** (1) All patients underwent CT examination before operation, and histopathology after operation confirmed other lesions with non-fungal balls in unilateral or bilateral maxillary sinus. (2) The CT diagnosis of the subjects showed that there was no obvious lesion in bilateral maxillary sinus.

**Exclusion criteria:** All cases have poor image quality (with artifacts or incomplete maxillary sinus photography).

A total of 107 cases were collected according to this criterion, and the basic information of the patients was shown in table 1.

**Table 1.** Basic data of patients with and without maxillary sinus fungal spheres.

Case characteristics	Fungal ball of maxillary sinus	Non-maxillary sinus fungus balls			P
		Other maxillary sinus diseases	Healthy maxillary sinuses	Total number	
Number of cases	47	30	30	60	-
Gender	Male	17	21	40	P=0.002 *
	Female	30	9	20	
Age (years)	57.0±12.4	52.6±16.1	44.1±13.8	48.4±15.5	P=0.002 *
Minimum (years)	30.0	21.0	20.0	20.0	-
Maximum (years)	80.0	81.0	75.0	81.0	
Median (years)	59.0	55.0	42.5	48.0	

### Construction and annotation of data sets

In this study, 107 cases were collected, of which 47 were positive, and the total number of CT sections was 6602. 60 cases were negative, and the total number of slides was 8205.

Firstly, 12 cases and 20 cases were randomly selected from the positive group and the negative group respectively to construct the test set. The test set was taken out at the beginning of the research to confirm that it is invisible in the establishment of algorithm model, thus ensuring the objectivity and authenticity of the algorithm model testing.

### Classification of data sets

The remaining portion of positive and negative cases after taking out the test set cases was used to construct the training set and the validation set in an 80/20 ratio (28 positive cases and 32 negative cases

as the training set, 7 positive cases and 8 negative cases as the validation set).

The classification data set was classified and marked by senior doctors, including the number of cases, the number of slides and other statistical information, as shown in table 2.

**Table 2.** The composition of the classified data set.

Classification dataset	Type and number of cases	Number of CT slices		
		including maxillary sinus	excluding maxillary sinus	Total
Training set	28 positive cases	1364	2547	3911
	32 negative cases	1560	2657	4217
Verification set	7 positive cases	361	618	979
	8 negative cases	401	711	1112
Test set	12 positive cases	555	1157	1712
	20 negative cases	1087	1789	2876
<b>Total</b>	<b>107 cases</b>	<b>5328</b>	<b>9479</b>	<b>14807</b>

**Detection of datasets**

The slices of the case were screened by senior doctors to construct the detection data set in line with the previous classification method. The slice source and quantity of positive and negative samples of each sub-data set are shown in table 3.

**Table 3.** Composition of test dataset.

Detection dataset	Positive slices		Negative slices		Total negative slices
	Slice feature	Number of slices	Slice feature	Number of slices	
Training set	Including maxillary sinus fungal balls	1001	Other maxillary sinus slices without maxillary sinus fungal balls	1923	2923
			Partial slices without maxillary sinus	1000	
Verification set	Including maxillary sinus fungal balls	212	Other maxillary sinus slices without maxillary sinus fungal balls	550	1050
			Partial slices without maxillary sinus	500	
Test set	Including maxillary sinus fungal balls	409	Other maxillary sinus slices without maxillary sinus fungal balls	1233	2233
			Partial slices without maxillary sinus	1000	
<b>Total</b>		<b>1622</b>		<b>6206</b>	

**Data annotation**

Based on the pathological results and clinical experience, two senior doctors used bounding boxes to cross-label the data of the lesions. A small amount of data with inconsistent labeling shall be reviewed and determined by the chief physician.

**Image preprocessing**

The CT data in this study were stored in DICOM (Digital Imaging and Communications in Medicine) format. The CT data were loaded using SimpleITK in Ubuntu 20.04 and Python 3.8, saving as 512×512 pixel slices at the selected window position and width.

The verification and test datasets were constructed according to the previously described method of constructing datasets. The image size of the verification dataset was adjusted to 224×224 pixels, and the image size of test dataset was maintained to 512×512 pixels. Figure 1 shows some typical examples of verification datasets.

Figure 2 shows some typical samples of the test dataset and their annotation information.

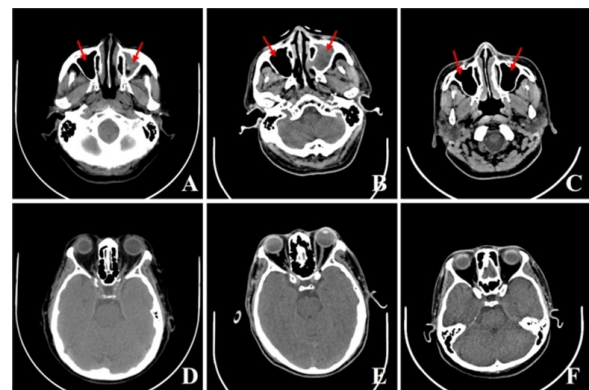


**Figure 1.** Partial sample of the verification dataset. Positive slices containing maxillary sinus: (A) Maxillary sinus fungus spheres; (B) Bacterial maxillary sinusitis; (C) Healthy maxillary sinuses; Corresponding negative slices without maxillary sinuses: (D), (E) and (F).

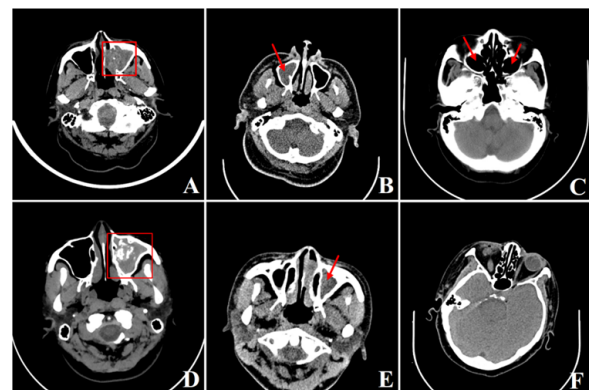


**Figure 2.** Positive sections containing fungal bulb lesions in the maxillary sinus: (A) and (D); Sections of the maxillary sinus excluding fungal bulb lesions: (B) Inverted papilloma; (E) Bacterial sinusitis nasal polyps; (C) Healthy maxillary sinus; (F) Non-maxillary sinus sections. The red bounding box represents the marked fungal ball lesion in the maxillary sinus.

### Methods of deep learning

In this study, a two-stage diagnostic method for maxillary sinus fungal spheres based on 2D CNN was proposed. The method consists of two stages. The first stage is a classification model, which classifies CT sections according to whether they contain maxillary sinuses. Subsequently, the sections containing maxillary sinus selected for the first stage classification were examined and the lesions of maxillary sinus fungal spheres were located.

In terms of classification models, considering the relatively obvious features of the maxillary sinus in CT slices in this study, the VGG19 model was used for analysis. The size of the input image for the classification model was consistent with the common 224×224 pixels. The single-channel CT section was directly copied and expanded to three-channel as input to the model.

In terms of model detection, Faster-RCNN, which integrates FPN<sup>(20)</sup> (Feature Pyramid Networks), was selected. The network integrates multi-layer characteristics, and the model has good robustness, high speed and high precision. The input image size of the detection model uses the original 512×512 pixels, which was directly expanded from a single channel copy to a three-channel input.

A two-stage diagnosis method of maxillary sinus fungus ball is then constructed based on the above classification and detection model (figure 3).

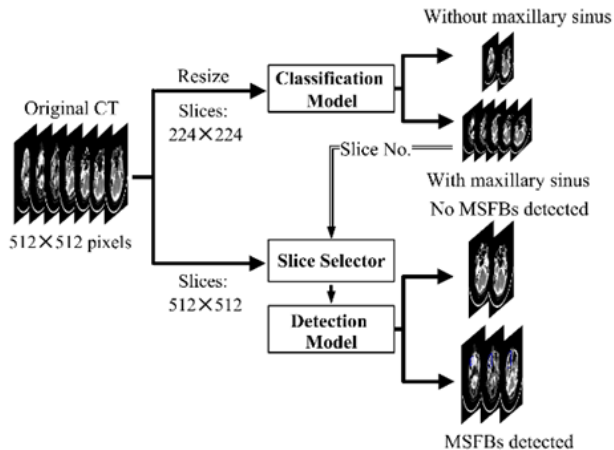


**Figure 3.** Flow chart of two-stage auxiliary diagnosis method for fungal ball in maxillary sinus. MSFBs: Maxillary Sinus Fungal Balls.

### Statistical Methods

IBM SPSS Statistics 26 was applied for statistical process. Shapiro wilk test was used to analyze the normality of measurement data. The comparison between patients' genders was conducted chi square analysis, while the comparison between ages was conducted by two independent sample *t*-tests. The diagnostic efficiency of the three methods was evaluated by calculating the area under the curve (AUC) by using the receiver's operating characteristic (ROC) curve. F-test was used to compare the time difference of the three diagnostic methods, and

Tamhane method was used to make multiple comparisons.

## RESULTS

In this study, a two-stage auxiliary diagnosis method for maxillary sinus fungal spheres based on 2D CNN fusion classification and detection model was proposed. This method used CT data and was based on the construction of deep convolution neural network. The training of deep convolutional neural network was carried out in Ubuntu 20.04 environment. A new environment space with Anaconda was created, where Python version was 3.8 and SimpleITK version was 2.0.1. The model was created and trained with PyTorch, version 1.8.0, and the corresponding version of torchvision was 0.9.0. A GPU was used for acceleration, the model was GTX1080 Ti, CUDA version 10.2, cuDNN version 8.0.5.

The classification model used a transfer based learning method, which was based on ImageNet pre-trained models and fine tuned on the maxillary sinus fungal ball dataset. The SGD optimizer with weight decay of 0.0001 and momentum of 0.9 was used for optimization. The Batch size was 128, the training was 30 rounds, and the initial learning rate was set to 0.01, which was reduced to 0.001 after 20 rounds and 0.0001 after 25 rounds. The training results of the classification model are listed in table 4. In the training process, early stopping was adopted to timely stop the training to prevent overfitting. The accuracy of the final classification model was 92.71%.

**Table 4.** Results of the classification model.

Model	Train		Verify		Test	
	Accuracy	Loss	Accuracy	Loss	Accuracy	Loss
VGG19	98.23	0.0453	96.11	0.062	92.71	0.102

The detection model was also trained by transfer learning. Based on the Faster-RCNN model pre-trained by the data set based on COCO, the data set of maxillary sinus fungus balls was further fine-tuned. According to experience, the training of the detection model was set to 25 rounds, and early stopping was also adopted to timely stop the training to prevent over fitting.

IoU is the intersection ratio between two bounding box representing the true value and the predicted value, which is often used to evaluate the detection effect of detection algorithms. See equation (1) for details:

$$IoU = \frac{Intersection(B_T, B_P)}{Union(B_T, B_P)} \quad (1)$$

Where;  $B_T$  and  $B_P$  are the bounding boxes of the true value and the predicted value respectively.

Since the detection results are usually only for doctors' reference, AP50 with IoU greater than 0.5 between the detection results of the detection model and the real value is given priority as the evaluation

index. Therefore, the results are shown in the detection results of Faster-RCNN in Table 5. The model based on Faster-RCNN can obtain 0.73 mAP and 0.76 AP50 on the test set.

**Table 5.** Detection results of Faster-RCNN.

Dataset	Faster-RCNN	
Training set	mAP	0.761
	AP50	0.78
Training set	mAP	0.759
	AP50	0.79
Test set	mAP	0.730
	AP50	0.76

The auxiliary diagnostic method of maxillary sinus fungal spheres was obtained through the cascade of classification and detection model. Firstly, the classification model classified each section of CT data, and screened out the section containing maxillary sinus. Subsequently, the detection model was used to detect lesions in the classified sections. If there was more than or equal to 1 slice with maxillary sinus fungal ball lesion detected and located, the CT case would be defined as maxillary sinus fungal ball. If no corresponding lesion was detected, the case shall defined as having no maxillary sinus fungal ball.

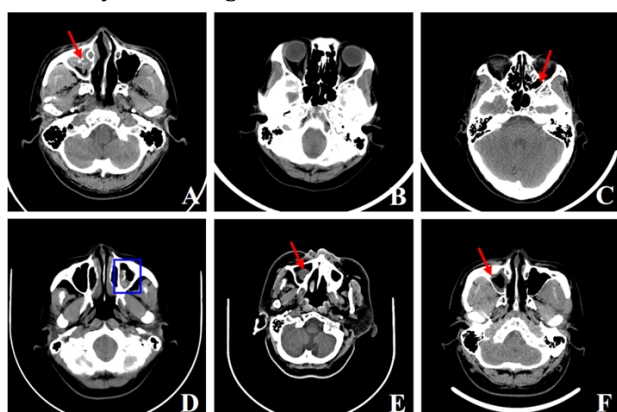


**Figure 4.** (A) The correct positive slice containing maxillary sinus; (B) The correct negative slice without maxillary sinus; (C) The wrong slice without maxillary sinus; (D) The correct positive slice containing fungal ball of maxillary sinus (the blue box in the figure is the detection result); (E) The correct negative section which does not contain fungal ball of maxillary sinus; (F) The slice containing fungal balls of maxillary sinus but detected incorrectly.

Figure 4 shows an example of correct and incorrect slices for classification and detection model diagnosis.

The diagnosis method was compared with that of doctors. Firstly, the test set was classified and checked out by this method, and the results were recorded. Secondly, four doctors were selected, including one senior radiologist and one junior radiologist, and one senior otolaryngologist and one junior otolaryngologist. The selection criteria for doctors with high seniority are those who have obtained intermediate title or above and worked for more than 10 years, while the selection criteria for

doctors with low seniority are those who have obtained junior title and worked for less than 2 years. Doctors with the same years of experience were divided into one group, and the two groups of doctors recognized and judged the images of the test set respectively, and recorded their diagnosis results and the time required to diagnose each case. The results of three diagnostic approaches to the test set are compared as follows:

**Comparison of results of three diagnostic methods**

With pathological results as the gold standard, the slices of 32 cases in the test set were detected or read by this auxiliary diagnostic method and doctors with high and low experience. The diagnostic results of the three methods for each case are listed in table 6.

The diagnostic accuracy of this auxiliary method was 84.4%, and that of senior and junior doctors were 81.3% and 71.9% respectively. ROC curves and corresponding AUC of the three methods are shown in figure 5. AUC of this auxiliary method, senior doctors and junior doctors are 0.871, 0.817 and 0.708, respectively. By comparison, the diagnostic efficiency of this auxiliary method is higher than that of senior and junior doctors.

**Table 6.** Confusion matrix of results of three diagnostic methods.

True label	Algorithm		Senior doctors		Junior doctors	
	Maxillary sinus fungus balls	Non-maxillary sinus fungus balls	Maxillary sinus fungus balls	Non-maxillary sinus fungus balls	Maxillary sinus fungus balls	Non-maxillary sinus fungus balls
Maxillary sinus fungus balls	11	1	10	2	8	4
Non-maxillary sinus fungus balls	4	16	4	16	5	15

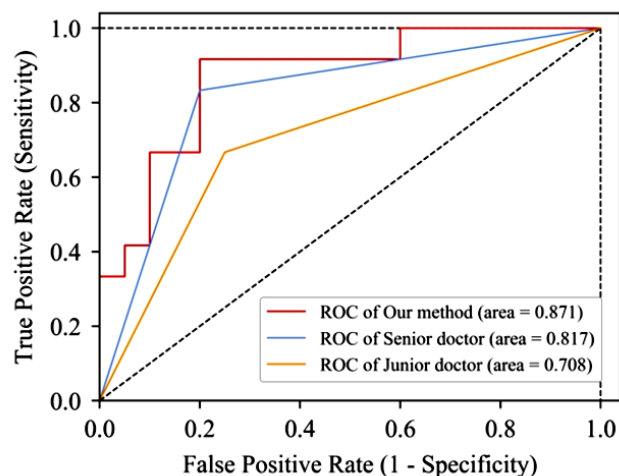


**Figure 5.** ROC curves and AUC of the three methods. ROC curves: The receiver’s operating characteristic curve; AUC: The area under the curve.

### Comparison of time consuming of three diagnostic methods

In the two-stage diagnosis method, the classification time of each case was  $10.46 \pm 3.21$  s by the classification model. The detection time of each case was  $8.86 \pm 1.68$  s. After synthesis, the diagnosis time of each case of the algorithm model is about  $32.03 \pm 5.83$  s. The average diagnostic time of senior and junior doctors was  $61.98 \pm 16.06$  s and  $99.85 \pm 17.11$  s, respectively. The results of ANOVA showed that the time consuming of the three diagnostic methods was significantly different ( $F=634.127$ ,  $P<0.001$ ). Tamhane multiple mean comparison results showed that the time spent in deep learning diagnosis was lower than that of senior and junior physicians, and there was a significant difference between the mean values ( $I-J=-29.95$ ,  $P<0.001$ ;  $I-J=-67.82$ ,  $P<0.001$ ).

## DISCUSSION

Based on a small number of data samples, a two-stage diagnosis method of maxillary sinus fungus ball is proposed based on deep convolution neural network, which consists of maxillary sinus slice classification model and maxillary sinus fungus ball lesion detection model. Studies have shown that this method has high classification and detection accuracy and good diagnostic effect. The establishment of the model does not require a large amount of data, and the training and deployment of the model requires little resources and is relatively convenient, which can provide certain help for doctors in the diagnosis of maxillary sinus fungal spheres.

When using a classification model to classify CT slices, this algorithm can filter out slices containing the maxillary sinus, with high classification accuracy and fast classification speed. Some slices with good classification results are shown in figure 4A and figure 4B in our results. Figure 4C shows the case model of misclassification in which part of the ethmoid sinus was misidentified as the maxillary sinus.

When the detection model is used to detect the fungal globular lesions of maxillary sinus, the lesions can be accurately located. Some slices with good detection results and problems are shown in figure 4D, E, F, and the blue box marks the detection results of the detection model. In the figure, D and E are the correct sections detected. It can be seen that D is the maxillary sinus fungal sphere section and E is the maxillary sinus cyst section. The characteristics of maxillary sinus fungal sphere with or without maxillary sinus are very obvious in the section, and the model has correctly diagnosed them. F is the section with the wrong detection. In this case, the maxillary sinus fungal sphere lesions were small, and the lesion features in some sections containing

maxillary sinus were not typical, so the model misjudged them as non-maxillary sinus fungal sphere slices. Therefore, although 2D network has certain advantages compared with 3D, it still has some congenital defects compared with 3D analysis methods, resulting in some errors in the analysis. We will continue to analyze and improve this in the future.

In addition, the establishment of the model requires a lot of data, and the maxillary sinus fungal sphere data requires pathological confirmation, which is usually difficult to collect. However, the establishment of the algorithm model should cover a variety of cases as far as possible, especially those cases with similar CT characteristics of maxillary sinus fungal spheres. In the future, these data can be included for further iteration to further improve the robustness and generalization of the model. Further research aims at clinical application, and creates more accurate deep learning models by increasing training data sets, including images obtained from other facilities. In the future, we will expand various data sets and train the model to provide assistance for lesion detection in other images, such as renal parenchymal tumor images, liver tumor images and cardiac coronary sinus morphological images.

The main contributions of this study are as follows: First, the data set of maxillary sinus fungal spheres was initially established and the inclusion criteria of corresponding cases were specified. Second, this study explored the application of deep convolutional neural network method in maxillary sinus fungal sphere assisted diagnosis. Third, this study analyzes other ways to analyze CT data besides 3D convolutional neural network.

In summary, the development of a two-stage assistive diagnostic method for maxillary sinus fungal balls based on deep learning is feasible and holds the potential to enhance the accuracy and efficiency of the diagnostic process for maxillary sinus lesions.

**Conflict of Interests:** The authors declared no conflict of interest.

**Ethical consideration:** This study was approved by the Ethics Committee of Zhoupu Hospital, Pudong New Area, Shanghai. (Approval number: 2022-C-136-E01, review date: 2022-08-11).

**Fund:** Shanghai University of Medicine & Health Sciences Affiliated Zhoupu Hospital 2023 Hospital-level Talent Project (ZPRC-2023A-09); Health and Family Planning Research Project of Pudong New Area Health Committee (PW2021A-80) and Cross Disciplinary Research Fund of Shanghai JiaoTong University (YG2021ZD16).

**Authors' contributions:** LP and LZ designed the study and performed the experiments, QW and RS collected the data, HK, WL and WD analyzed the data, LP and LZ prepared the manuscript. All authors read and approved the final manuscript.

## REFERENCES

1. Alshaiikh NA, Alshiha KS, Yeak S, Lo S (2020) Fungal Rhinosinusitis: Prevalence and Spectrum in Singapore. *Cureus*, **12**(4): e7587.
2. Grosjean P and Weber R (2007) Fungus balls of the paranasal sinuses: a review. *European Archives of Oto-Rhino-Laryngology*, **264**(5): 461-470.
3. Ho CF, Lee TJ, Wu PW, et al. (2019) Diagnosis of a maxillary sinus fungus ball without intralesional hyperdensity on computed tomography. *Laryngoscope*, **129**(5): 1041-1045.
4. Lee DH, Yoon TM, Lee JK, Lim SC (2020) Computed tomography-based differential diagnosis of fungus balls in the maxillary sinus. *Oral Surgery Oral Medicine Oral Pathology Oral Radiology*, **129**(3): 277-281.
5. Gupta K and Saggarr K (2014) Analysis of computed tomography features of fungal sinusitis and their correlation with nasal endoscopy and histopathology findings. *Annals of African Medicine*, **13**(3): 119-123.
6. Pirner S, Tingelhoff K, Wagner I, et al. (2009) CT-based manual segmentation and evaluation of paranasal sinuses. *Eur Arch Otorhinolaryngol*, **266**(4): 507-518.
7. Abrol A, Bhattarai M, Fedorov A, et al. (2020) Deep residual learning for neuroimaging: An application to predict progression to Alzheimer's disease. *J Neurosci Methods*, **339**: 108701.
8. Shin HC, Roth HR, Gao M, et al. (2016) Deep convolutional neural networks for computer-aided detection: CNN architectures, dataset characteristics and transfer learning. *IEEE Trans Med Imaging*, **35**(5): 1285-1298.
9. Chen X, Zhang K, Lin S, et al. (2021) Single shot multibox detector automatic polyp detection network based on gastrointestinal endoscopic images. *Comput Math Methods Med*. **2021**: 2144472.
10. Ghesu FC, Georgescu B, Zheng Y, et al. (2019) Multi-Scale Deep Reinforcement Learning for Real-Time 3D-Landmark Detection in CT Scans. *IEEE Trans Pattern Anal Mach Intell*, **41**(1):176-189.
11. Ren S, He K, Girshick R, Sun J (2017) Faster R-CNN: Towards real-time object detection with region proposal networks. *Ieee Transactions On Pattern Analysis and Machine Intelligence*, **39**(6): 1137-1149.
12. Shelhamer E, Long J and Darrell T (2017) Fully Convolutional Networks for Semantic Segmentation. *Ieee Transactions On Pattern Analysis and Machine Intelligence*, **39**(4): 640-651.
13. Venkadesh KV, Setio A, Schreuder A, et al. (2021) Deep learning for malignancy risk estimation of pulmonary nodules detected at low-dose screening CT. *Radiology*, **300**(2): 438-447.
14. Zhou Q, Xue C, Ke X, Zhou J (2022) Treatment Response and Prognosis Evaluation in High-Grade Glioma: An Imaging Review Based on MRI. *J Magn Reson Imaging*, **56**(2): 325-340.
15. Jamshidi MB, Labakhsh A, Talla J, et al. (2020) Artificial intelligence and COVID-19: Deep learning approaches for diagnosis and treatment. *IEEE Access*, **8**(109581-109595).
16. Kim Y, Lee KJ, Sunwoo L, et al. (2019) Deep Learning in Diagnosis of Maxillary Sinusitis Using Conventional Radiography. *Investigative Radiology*, **54**(1): 7-15.
17. Murata M, Arijji Y, Ohashi Y, et al. (2019) Deep-learning classification using convolutional neural network for evaluation of maxillary sinusitis on panoramic radiography. *Oral Radiology*, **35**(3): 301-307.
18. Xu J, Wang S, Zhou Z, et al. (2020) Automatic CT image segmentation of maxillary sinus based on VGG network and improved V-Net. *International Journal of Computer Assisted Radiology and Surgery*, **15**(9): 1457-1465.
19. Kim KS, Kim BK, Chung MJ, et al. (2022) Detection of maxillary sinus fungal ball via 3-D CNN-based artificial intelligence: Fully automated system and clinical validation. *Plos One*, **17**(2): e263125.
20. Min K, Lee GH, Lee SW (2022) Attentional feature pyramid network for small object detection. *Neural Netw*, **155**: 439-450.

